AMERICAN SOCIETY FOR MICROBIOLOGY | Applied and Environmental Microbiology®

BIODEGRADATION

Hydrolase CehA and Monooxygenase CfdC Are Responsible for Carbofuran Degradation in *Sphingomonas* sp. Strain CDS-1

Xin Yan,[a,c] Wen Jin,[a] Guang Wu,[a] Wankui Jiang,[a] Zhangong Yang,[a] Junbin Ji,[a] Jiguo Qiu,[a] Jian He,[a,b] Jiandong Jiang,[a] Qing Hong[a]

[a]Key Laboratory of Agricultural Environmental Microbiology, Ministry of Agriculture, College of Life Sciences, Nanjing Agricultural University, Nanjing, Jiangsu, People's Republic of China

[b]Laboratory Center of Life Sciences, College of Life Sciences, Nanjing Agricultural University, Nanjing, Jiangsu, People's Republic of China

[c]Jiangsu Provincial Key Lab for Organic Solid Waste Utilization, Nanjing Agricultural University, Nanjing, Jiangsu, People's Republic of China

ABSTRACT Carbofuran, a broad-spectrum systemic insecticide, has been extensively used for approximately 50 years. Diverse carbofuran-degrading bacteria have been described, among which sphingomonads have exhibited an extraordinary ability to catabolize carbofuran; other bacteria can only convert carbofuran to carbofuran phenol, while all carbofuran-degrading sphingomonads can degrade both carbofuran and carbofuran phenol. However, the genetic basis of carbofuran catabolism in sphingomonads has not been well elucidated. In this work, we sequenced the draft genome of *Sphingomonas* sp. strain CDS-1 that can transform both carbofuran and carbofuran phenol but fails to grow on them. On the basis of the hypothesis that the genes involved in carbofuran catabolism are highly conserved among carbofuran-degrading sphingomonads, two such genes, $cehA_{CDS-1}$ and $cfdC_{CDS-1}$, were predicted from the 84 open reading frames (ORFs) that share ≥95% nucleic acid similarities between strain CDS-1 and another sphingomonad *Novosphingobium* sp. strain KN65.2 that is able to mineralize the benzene ring of carbofuran. The results of the gene knockout, genetic complementation, heterologous expression, and enzymatic experiments reveal that $cehA_{CDS-1}$ and $cfdC_{CDS-1}$ are responsible for the conversion of carbofuran and carbofuran phenol, respectively, in strain CDS-1. $CehA_{CDS-1}$ hydrolyzes carbofuran to carbofuran phenol. $CfdC_{CDS-1}$, a reduced flavin mononucleotide ($FMNH_2$)- or reduced flavin adenine dinucleotide ($FADH_2$)-dependent monooxygenase, hydroxylates carbofuran phenol at the benzene ring in the presence of NADH, FMN/FAD, and the reductase CfdX. It is worth noting that we found that carbaryl hydrolase $CehA_{AC100}$, which was previously demonstrated to have no activity toward carbofuran, can actually convert carbofuran to carbofuran phenol, albeit with very low activity.

IMPORTANCE Due to the extensive use of carbofuran over the past 50 years, bacteria have evolved catabolic pathways to mineralize this insecticide, which plays an important role in eliminating carbofuran residue in the environment. This study revealed the genetic determinants of carbofuran degradation in *Sphingomonas* sp. strain CDS-1. We speculate that the close homologues *cehA* and *cfdC* are highly conserved among other carbofuran-degrading sphingomonads and play the same roles as those described here. These findings deepen our understanding of the microbial degradation mechanism of carbofuran and lay a foundation for the better use of microbes to remediate carbofuran contamination.

KEYWORDS hydrolase CehA, carbofuran, monooxygenase CfdC, sphingomonads, upstream catabolic pathway

Received 6 April 2018 **Accepted** 31 May 2018

Accepted manuscript posted online 8 June 2018

Citation Yan X, Jin W, Wu G, Jiang W, Yang Z, Ji J, Qiu J, He J, Jiang J, Hong Q. 2018. Hydrolase CehA and monooxygenase CfdC are responsible for carbofuran degradation in *Sphingomonas* sp. strain CDS-1. Appl Environ Microbiol 84:e00805-18. https://doi.org/10.1128/AEM.00805-18.

Editor Rebecca E. Parales, University of California, Davis

Address correspondence to Qing Hong, hongqing@njau.edu.cn.

Carbofuran (2,3-dihydro-2,2-dimethyl-7-benzofuranoyl-*N*-methylcarbamate), a representative broad-spectrum *N*-methylcarbamate pesticide (Fig. 1A), was first introduced in 1967 by the FMC Corporation (Princeton, NJ, USA). Carbofuran was widely used to control insect and nematode pests in crops (1). Carbofuran is a potent inhibitor of cholinesterase in mammals (2, 3). Moreover, the pesticide also acts as an endocrine disruptor (4). Therefore, carbofuran was prohibited in many countries, but it is still used in some developing countries due to its insecticidal effects. Although carbofuran is not stable chemically because of hydrolysis in the environment, its relatively good water solubility (700 mg/liter at 25°C) and low adsorption (mean organic carbon-water partition coefficient [K_{oc}] of 30) (https://www3.epa.gov/pesticides/endanger/litstatus/effects/carbofuran/riskanalysis.pdf) result in the contamination of surface and groundwater. Therefore, great concern and interest have been raised regarding the environmental behavior and degradation mechanisms of carbofuran.

Microbial degradation plays an important role in the elimination of carbofuran in the environment. Various carbofuran-degrading microbes, mostly bacteria and some fungi, have been isolated from diverse geographical origins. The reported carbofuran-degrading bacteria are from the genera *Pseudomonas*, *Flavobacterium*, *Achromobacter*, *Sphingomonas*, *Novosphingobium*, and *Paracoccus* (5–14). Among these bacteria, only sphingomonads (bacteria of the genus *Sphingomonas* and the closely related genera *Novosphingobium*, *Sphingopyxis*, and *Sphingobium*, commonly referred to as sphingomonads [15, 16]) can covert carbofuran to carbofuran phenol and further transform carbofuran phenol (8, 10–13), while others just perform the hydrolysis of carbofuran to carbofuran phenol. In the *Sphingomonas* sp. strain SB5, it was proposed that following the production of carbofuran phenol, a putative hydrolase has the ability to catalyze the cleavage of the furanyl ring (10). Recently, the complete catabolic pathway of carbofuran mineralization by strain KN65.2 was proposed according to the metabolic profiling of wild-type KN65.2 and its plasposon mutants (Fig. 1A) (13); in strain KN65.2, carbofuran phenol is likely hydroxylated by a monooxygenase described below, leading to the cleavage of the furanyl ring. Here, the catabolic pathways before and after the cleavage of the benzene ring are called the upstream pathway and the downstream pathway, respectively.

The genetic basis of the carbofuran catabolic pathway is far from clear. Two carbofuran hydrolases, Mcd and CfdJ, which catalyze the conversion of carbofuran to carbofuran phenol, have been reported. Mcd was purified from *Achromobacter* sp. strain WM111, and the corresponding gene *mcd* was cloned (17). The homologues of *mcd* have been detected in phylogenetically diverse carbofuran-degrading isolates (18), but no *mcd* homologue has been found in carbofuran-degrading sphingomonads. *cfdJ* was found in the genome of *Novosphingobium* sp. strain KN65.2 (19), which is a close homologue of the carbaryl hydrolase-encoding gene *cehA* cloned from the *Rhizobium* sp. strain AC100. $CehA_{AC100}$ catalyzes the conversion of carbaryl to 1-naphthol (20). Although $CehA_{KN65.2}$ (CfdJ is the same as $CehA_{KN65.2}$) and $CehA_{AC100}$ differ by only four amino acids, $CehA_{KN65.2}$ but not $CehA_{AC100}$ can recognize carbofuran as a substrate (20, 21). Hashimoto et al. found that $CehA_{AC100}$, purified from the *Rhizobium* sp. strain AC100, showed no detectable activity against carbofuran (20). Öztürk et al. revealed that none of the $CehA_{KN65.2}$ amino acid residues that differ from $CehA_{AC100}$ were silent regarding carbofuran hydrolytic activity, but the substitution of Phe152 to Leu152 proved crucial (21). Therefore, it is likely that the close homologues of *cehA* are responsible for the conversion of carbofuran to carbofuran phenol in carbofuran-degrading sphingomonads, although this must be further confirmed by genetic evidence.

To identify the genes involved in the mineralization of carbofuran in strain KN65.2, Nguyen et al. generated 27 plasposon mutants of strain KN65.2, which abolished or diminished its capability to degrade and mineralize carbofuran (13). On the basis of the results of metabolite analysis of the mutants and sequence analysis of the genes disrupted by mini-Tn*5*, it was proposed that the gene cluster *cfdABCDEFGH* is involved in the mineralization of carbofuran phenol. CfdC is predicted to be a flavin-dependent

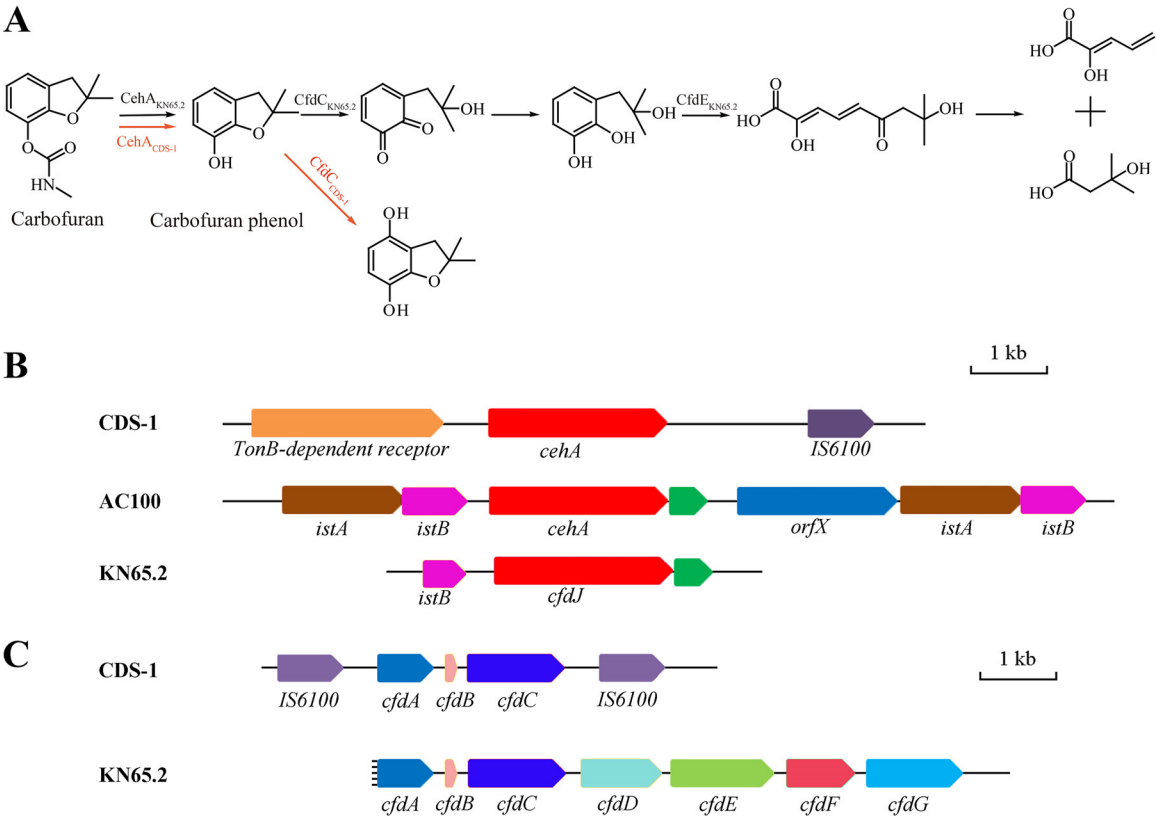

FIG 1 Catabolism of carbofuran in strains *Novosphingobium* sp. KN65.2 and *Sphingomonas* sp. CDS-1 and genomic context of *cehA* and *cfdC* in different hosts. (A) Tentative catabolic pathway of carbofuran in strains *Novosphingobium* sp. KN65.2 (black arrows) and *Sphingomonas* sp. CDS-1 (red arrows). Strains KN65.2 and CDS-1 are able to transform both carbofuran and carbofuran phenol (11, 13). Strain KN65.2 can also cleave the aromatic moiety of carbofuran and further degrade the cleaved aromatic ring. Strain CDS-1 failed to break the aromatic moiety and cannot grow on carbofuran. CehA and CfdC are responsible for the initial two steps of carbofuran catabolism. $CfdE_{KN65.2}$ supposedly catalyzes the cleavage of the benzene ring of carbofuran in strain KN65.2 (13). Notably, the proposed products of carbofuran phenol catalyzed by CfdC are different in strains KN65.2 and CDS-1. (B) Genomic context of *cehA* in strains *Sphingomonas* sp. CDS-1, *Rhizobium* sp. AC100 (20), and *Novosphingobium* sp. KN65.2 (21). (C) Genomic context of *cfdC* in strains *Sphingomonas* sp. CDS-1 and *Novosphingobium* sp. KN65.2 (13). The nearly identical ORFs are drawn in the same color.

monooxygenase, and CfdE is a putative dioxygenase; CfdC and CfdE may be responsible for the hydroxylation and the cleavage of the benzene ring of carbofuran phenol, respectively. However, more genetic and biochemical data are needed to validate the functional and physiological roles of CfdC and CfdE.

The *linABCDEF* genes for the catabolism of hexachlorocyclohexane (HCH) are found in the HCH-mineralizing sphingomonads isolated all over the world (22). Similarly, the genes involved in the isoproturon-catabolic pathway are highly conserved among the isoproturon-mineralizing sphingomonads (23). Considering these facts, we hypothesized that the genes involved in carbofuran catabolism might also be conserved (likely with >95% similarity) among carbofuran-degrading sphingomonads. Both *Sphingomonas* sp. strain CDS-1 and *Novosphingobium* sp. strain KN65.2 can convert carbofuran and carbofuran phenol (11, 13). However, unlike strain KN65.2, strain CDS-1 cannot utilize carbofuran or carbofuran phenol as a sole carbon source for growth. Strain CDS-1 was isolated from activated sludge in the Jiangsu province of China, and strain KN65.2 was isolated from soil sampled from a vegetable field with a long history of carbofuran treatment in the Soc Trang province of Vietnam. The draft genome sequence of strain KN65.2 was released recently (19). In this work, the draft genome of strain CDS-1 was sequenced; the genes involved in the carbofuran catabolism were first predicted from the open reading frames (ORFs) that share ≥95% nucleic acid similarities between strains CDS-1 and KN65.2 and then were subjected to experimental validation.

RESULTS

Prediction of carbofuran catabolic genes via comparative genomic analysis. The draft genome sequence of strain CDS-1 contains 409 contigs, constituting a total size of 5.37 Mb (5,244 ORFs), of which the G+C content is 62.7%. A total of 84 ORFs sharing ≥95% nucleic acid similarities between the genomes of strains CDS-1 and KN 65.2 were found (see Table S1 in the supplemental material). Then, the candidate genes involved in the catabolism of carbofuran were predicted from these 84 ORFs. Similar to strain KN65.2, strain CDS-1 lacks *mcd* but harbors a close homologue of $cehA_{AC100}$. As shown in Fig. 1B, $cehA_{AC100}$ is located on a mobile genetic element (Tn*ceh*) bordered by two insertion sequence (IS) elements, each of which contains a transposase gene pair (*istA-istB*). Only partial Tn*ceh* carrying a truncated *istB*, $cehA_{KN65.2}$, and a short ORF following $cehA_{KN65.2}$ are retained in strain KN65.2. In contrast, besides $cehA_{CDS-1}$, no additional Tn*ceh* sequences were found in the contig containing $cehA_{CDS-1}$. The ORF upstream of $cehA_{CDS-1}$ encodes a putative TonB-dependent receptor, and an IS element (IS*6100*) is located downstream of $cehA_{CDS-1}$. There is only one amino acid (Phe152Leu) different between $CehA_{AC100}$ and $CehA_{CDS-1}$, while $CehA_{CDS-1}$ and $CehA_{KN65.2}$ differ from each other at three amino acid residues, Gly or Ala (207), Thr or Ala (494), and Ile or Thr (570). It was demonstrated that $CehA_{AC100}$ showed no hydrolytic activity toward carbofuran and gained this ability through the substitution of Leu152 for Phe152 (21). Therefore, $cehA_{CDS-1}$ is likely responsible for the conversion of carbofuran to carbofuran phenol in strain CDS-1.

Among the genes in cluster *cfdABCDEFGH* from strain KN65.5, only *cfdABC* was found in the genome of strain CDS-1. As shown in Fig. 1C, *cfdABC* was organized in a mobile genetic element with IS*6100* at each side in strain CDS-1, while no IS element was found around *cfdABCDEFGH* in strain KN65.2. Since $cfdC_{CDS-1}$ and $cfdC_{KN65.2}$ share 99% nucleic acid similarity, we assumed that $cfdC_{CDS-1}$ is responsible for the hydroxylation of carbofuran phenol in strain CDS-1. Strain CDS-1 cannot grow on carbofuran or carbofuran phenol, and so it probably does not contain the genes for the downstream pathway of carbofuran catabolism. Since no other candidate genes involved in the catabolism of carbofuran were found among the 84 ORFs, this work focused on identifying the roles of $cehA_{CDS-1}$ and $cfdC_{CDS-1}$.

***cehA*$_{CDS-1}$ is responsible for the conversion of carbofuran to carbofuran phenol in strain CDS-1, and CehA$_{AC100}$ can recognize carbofuran as a substrate.** To determine its *in vivo* role, $cehA_{CDS-1}$ was inactivated through a single-crossover event as described in Materials and Methods. The mutant strain CDS-1-cehA lost the ability to transform carbofuran (Fig. 2A), which was restored by plasmid pBBR-cehA containing $cehA_{CDS-1}$. Since $CehA_{CDS-1}$ is the Phe152Leu substitution mutant of $CehA_{AC100}$ and the latter was demonstrated as being unable to hydrolyze carbofuran (20, 21), we investigated whether a Phe152Leu substitution enables $CehA_{AC100}$ to hydrolyze carbofuran. $CehA_{CDS-1}$ and $CehA_{AC100}$ were heterologously expressed in *Escherichia coli* and purified as N-terminal 6His-tagged fusion proteins. The sizes of the purified 6His-$CehA_{CDS-1}$ and 6His-$CehA_{AC100}$ closely matched the expected size (87.657 kDa) on the SDS-PAGE (see Fig. S1). According to the size exclusion chromatography analysis (see Fig. S2), 6His-$CehA_{CDS-1}$ existed as a dimer, which is in line with previous descriptions of $CehA_{AC100}$ purified from *Rhizobium* sp. strain AC100 (20). As shown in Table 1, the K_m, k_{cat}, and k_{cat}/K_m of 6His-$CehA_{CDS-1}$ for carbofuran were 230 ± 5.5 μM, 10.2 ± 0.8 s^{-1}, and (4.4 ± 0.3) × 10^{-2} $s^{-1} \cdot \mu M^{-1}$, respectively; the K_m, k_{cat} and k_{cat}/K_m of 6His-$CehA_{AC100}$ for carbofuran were 880 ± 9.0 μM, 0.7 ± 0.1 s^{-1}, and (0.8 ± 0.1) × 10^{-3} $s^{-1} \cdot \mu M^{-1}$, respectively. These data show that 6His-$CehA_{AC100}$ must be able to hydrolyze carbofuran to carbofuran phenol, albeit with much lower catalytic efficiency than 6His-$CehA_{CDS-1}$; a Phe152Leu substitution significantly enhances the activity of $CehA_{AC100}$ toward carbofuran.

***cfdC*$_{CDS-1}$ is in charge of the transformation of carbofuran phenol in strain CDS-1.** To investigate the physiological role of $cfdC_{CDS-1}$, a derivative of strain CDS-1 with the inactivation of $cfdC_{CDS-1}$ was constructed. The resulting mutant strain CDS-1-cfdC showed no detectable degrading activity toward carbofuran phenol (Fig. 2A), and

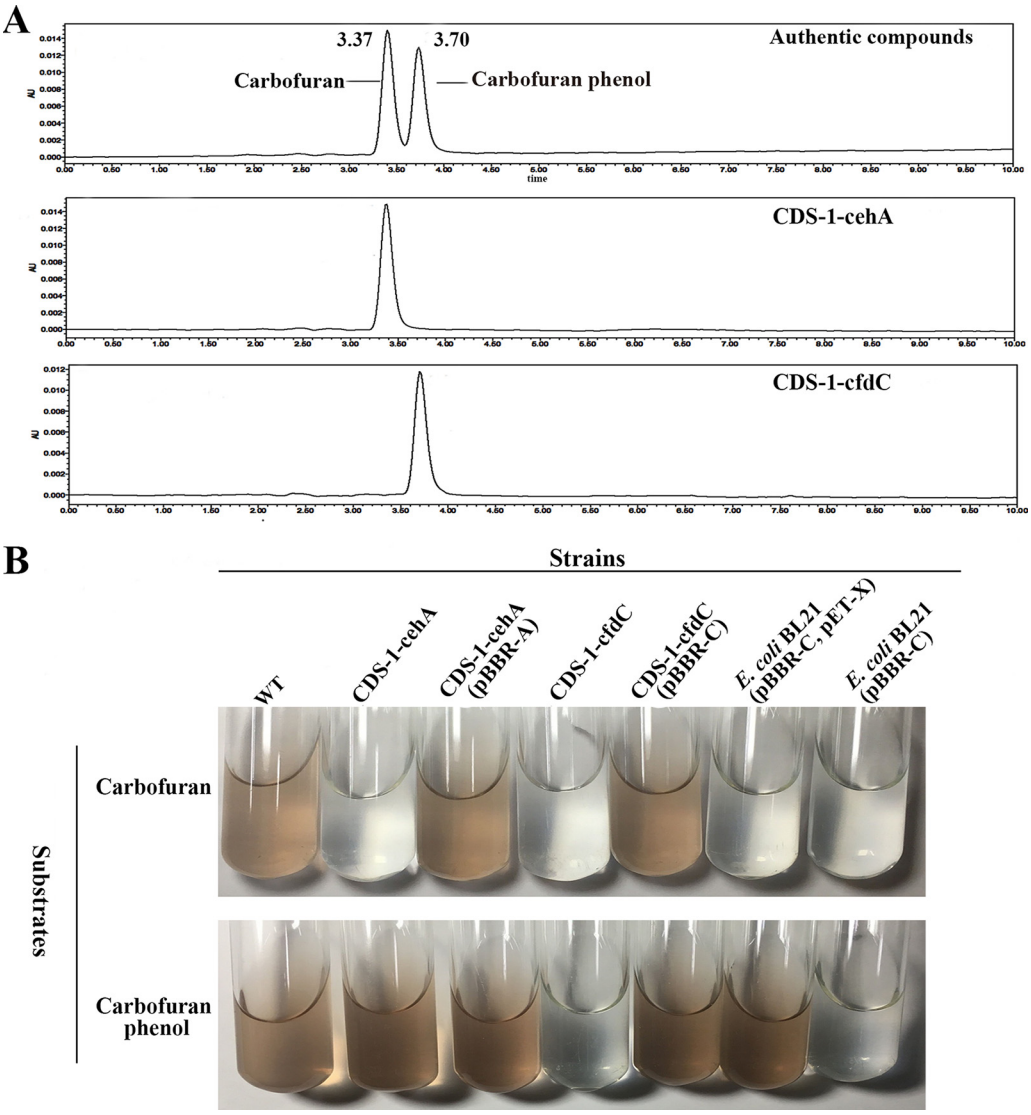

FIG 2 Transformation of carbofuran or carbofuran phenol by tested strains. WT, *Sphingomonas* sp. strain CDS-1; CDS-1-cehA, $cehA_{CDS\text{-}1}$-inactivated mutant of strain CDS-1; CDS-1-cfdC, *cfdC*-inactivated mutant of strain CDS-1. Plasmid pBBR-A contains $cehA_{CDS\text{-}1}$ and its putative promoter region. Plasmid pBBR-C carries *cfdC* and its putative promoter region. Plasmid pET-X harbors *cfdX* under the control of the T7 promoter. (A) HPLC analysis of the products of carbofuran degraded by strains CDS-1-cehA and CDS-1-cfdC. The degradation test is described in Materials and Methods. (B) Degradation of carbofuran and carbofuran phenol by the tested strains. The strains that can functionally express CfdC are able to transform carbofuran phenol and generate red compounds.

the $cfdC_{CDS\text{-}1}$-complemented mutant strain CDS-1-cfdC(pBBR-C) regained its ability to transform carbofuran phenol. In addition, carbofuran-degrading sphingomonads convert carbofuran phenol with the production of a red compound (8, 10, 13, 24). The mutant strain CDS-1-cfdC failed to produce a red compound in the presence of carbofuran phenol, which was restored by the introduction of plasmid pBBR-C (Fig. 2B). To further verify the function of $CfdC_{CDS\text{-}1}$, plasmid pBBR-C containing $cfdC_{CDS\text{-}1}$ under the control of its native promoter was introduced into strains *Sphingomonas wittichii* RW1 (25), *Pseudomonas putida* KT2440 (26), and *E. coli* DH5α. The plasmid pBBR-C conferred strains RW1 and KT2440 (data not shown) but not strain DH5α with the ability to transform carbofuran phenol (Fig. 2B). These results indicate that $cfdC_{CDS\text{-}1}$ is responsible for the further conversion of carbofuran phenol in strain CDS-1. The functional expression of $cfdC_{CDS\text{-}1}$ in different hosts shows that $CfdC_{CDS\text{-}1}$ employed the reductases of the hosts. In addition, the inability of strain DH5α(pBBR-C) to transform

TABLE 1 Kinetic parameters[a] of recombinant $CehA_{CDS-1}$, $CehA_{AC100}$, CfdX, and CfdC

Enzyme	Substrate	Cofactor(s)	K_m (μM)	k_{cat} (s^{-1})	k_{cat}/K_m ($s^{-1} \cdot \mu M^{-1}$)
$CehA_{CDS-1}$	Carbofuran		230 ± 5.5	10.2 ± 0.8	(4.4 ± 0.3) × 10^{-2}
$CehA_{AC100}$	Carbofuran		880 ± 9.0	0.7 ± 0.1	(0.8 ± 0.1) × 10^{-3}
CfdX	NADH	FMN	1.8 ± 0.1	29.1 ± 1.3	16.4 ± 1.0
	FMN	NADH	1.0 ± 0.1	30.1 ± 1.1	29.4 ± 1.1
	NADH	FAD	13.9 ± 0.1	20.8 ± 0.9	1.5 ± 0.1
	FAD	NADH	9.0 ± 0.6	15.3 ± 1.3	1.7 ± 0.2
CfdCX[b]	Carbofuran phenol	NADH, FMN	39.1 ± 2.8	(3.0 ± 0.3) × 10^{-1}	(7.5 ± 0.7) × 10^{-3}
	Carbofuran phenol	NADH, FAD	49.0 ± 2.5	(2.0 ± 0.2) × 10^{-1}	(4.0 ± 0.5) × 10^{-3}

[a]Kinetic experiments were performed at 30°C in Tris-HCl buffer (20 mM, pH 7.5) with a final volume of 1 ml; values are means ± standard deviations calculated from triplicate assays.
[b]Molar ratio of CfdC/CfdX is 25:1.

carbofuran phenol may have been due to the lack of proper reductase component or to the unsuccessful synthesis of $CfdC_{CDS-1}$.

Identifying a proper reductase component for $CfdC_{CDS-1}$. To construct the activity of $CfdC_{CDS-1}$ *in vitro*, we sought to screen a proper reductase component for $CfdC_{CDS-1}$ from strain CDS-1. $CfdC_{CDS-1}$ belongs to the group D flavin monooxygenases (Fig. 3A), which are enzymes with an acyl-coenzyme A (acyl-CoA) dehydrogenase fold (27). Large flavin mononucleotide (FMN)-specific reductase and small flavin reductase have been reported as the reductase components of group D flavin monooxygenases (28, 29). However, no such reductase-encoding gene was found among the 84 ORFs or in the immediate vicinity of $cfdC_{CDS-1}$. Five genes were predicted to encode the flavin reductase gene in the genome of strain CDS-1 (Fig. 3B). Each of these five putative flavin reductases was coexpressed with CfdC in *E. coli*. The two plasmids pET08340 (carrying gene CBW64_RS08340) and pET17905 (carrying gene CBW64_RS17905) enabled strain *E. coli* BL21(DE3)/pBBR-C to convert carbofuran phenol (data not shown). Since strain BL21(DE3)/pET17905/pBBR-C exhibited the highest carbofuran phenol reactivity (Fig. 2B), gene CBW64_RS17905 was named *cfdX*, and its product was used to construct the activity of $CfdC_{CDS-1}$ in the following experiment.

CfdCX catalyzes the monooxygenation of carbofuran phenol. (i) Expression and purification of CfdC and CfdX. Recombinant CfdC and CfdX were individually overexpressed in *E. coli* BL21(DE3) as N- and C-terminal 6His-tagged fusion proteins, respectively. SDS-PAGE analysis showed that the molecular masses of 6His-CfdC and CfdX-6His were approximately 43.136 kDa and 18.181 kDa (Fig. S2), respectively, in agreement with the molecular weights deduced from their amino acid sequences. The results of the size exclusion chromatography analysis (Fig. S2) showed that 6His-CfdC existed as a dimer, while CfdX-6His existed as a mixture of a monomer and a hexamer at a proportion of approximately 5:1 (data not shown).

(ii) Characterization of CfdX. The NAD(P)H-oxidizing activity of purified CfdX-6His was determined in the presence of FMN or flavin adenine dinucleotide (FAD). The kinetic parameters of CfdX-6His are summarized in Table 1. CfdX-6His showed no detectable activity toward NADPH in the presence of FMN or FAD. CfdX-6His exhibited a higher catalytic efficiency (k_{cat}/K_m) (approximately 10-fold) for NADH when FMN was used as the second substrate, indicating that FMN was a more favorable electron acceptor than FAD for CfdX-6His. When NADH was used as a second substrate, the catalytic efficiency (k_{cat}/K_m) of CfdX-6His for FMN was approximately 17-fold that for FAD.

(iii) Characterization of 6His-CfdC. As shown in Fig. 4A, purified 6His-CfdC and CfdX-6His were able to convert carbofuran phenol to two new metabolites. Before the kinetic assays of the purified enzyme, the optimal molar ratios of 6His-CfdC and CfdX-6His were determined. The amount of 6His-CfdC was kept constant at 1 μM, while CfdX-6His was increased from 0 to 60 nM. 6His-CfdC showed negligible activity toward carbofuran phenol in the absence of CfdX-6His. However, the activity increased rapidly with the addition of CfdX-6His. The maximal activity was achieved when CfdX-6His was added at 40 nM, indicating that the optimal molar ratio of 6His-CfdC and CfdX-6His was

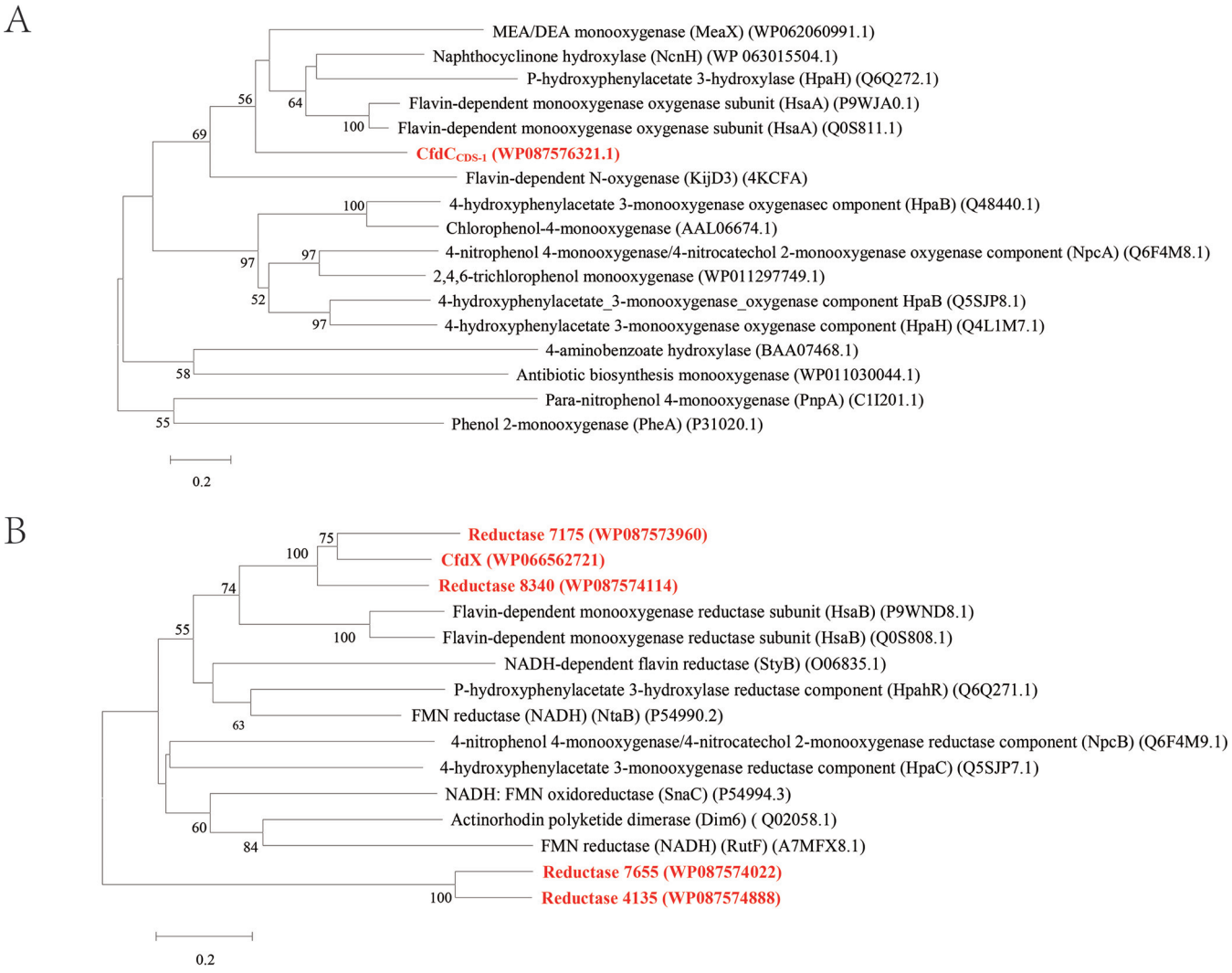

FIG 3 Phylogenetic analysis of CfdC$_{CDS-1}$ and the five flavin reductases predicted in *Sphingomonas* sp. strain CDS-1. (A) Phylogenetic comparison of CfdC$_{CDS-1}$ with selected group D flavin-dependent monooxygenases. (B) Phylogenetic tree of the five flavin reductases predicted in *Sphingomonas* sp. strain CDS-1 with selected flavin reductases. The multiple alignment analysis of the amino acid sequences was performed with Clustal X 2.1. The neighbor-joining method was used to construct the phylogenetic unrooted tree with MEGA 5.0. Protein identifiers (IDs) are shown at the end of each protein.

approximately 25:1 (Fig. 5). The kinetic assays revealed that the K_m and k_{cat}/K_m values of 6His-CfdC for carbofuran phenol were 39.1 $\pm$ 2.8 μM and (4.5 $\pm$ 0.4) $\times$ 10^{-1} $\mu M^{-} \cdot min^{-1}$, respectively. When FMN was replaced by FAD, the affinity and catalytic efficiency of 6His-CfdC for carbofuran phenol decreased slightly (Table 1).

(iv) CfdCX hydroxylates carbofuran phenol at the benzene ring. The two metabolites of carbofuran phenol catalyzed by purified 6His-CfdC and CfdX-6His were analyzed using high-performance liquid chromatography (HPLC) and tandem mass spectrometry (MS/MS) (Fig. 4). The molecular ion mass of metabolite 1 was *m/z* 181.0858 $[M+H]^+$, which is in line with the protonated derivative of hydroxylated carbofuran phenol ($C_{10}H_{13}O_3^+$, 181.0859) with a -0.55-ppm error (Fig. 4C). If carbofuran phenol was hydroxylated at the benzene ring by CfdCX, the resulting product may be prone to being oxidized to its corresponding quinone derivative. The molecular ion mass of metabolite 2 was *m/z* 179.0703 $[M+H]^+$, which is identical to the protonated derivative of this quinone compound ($C_{10}H_{11}O_3^+$, 179.0703) (Fig. 4D). Generally, a mass error between -5 ppm and 5 ppm is acceptable (30). Therefore, we proposed that CfdCX hydroxylates carbofuran phenol at the benzene ring. However, since this hydroxylated product is unstable, the attempt to identify it by nuclear magnetic

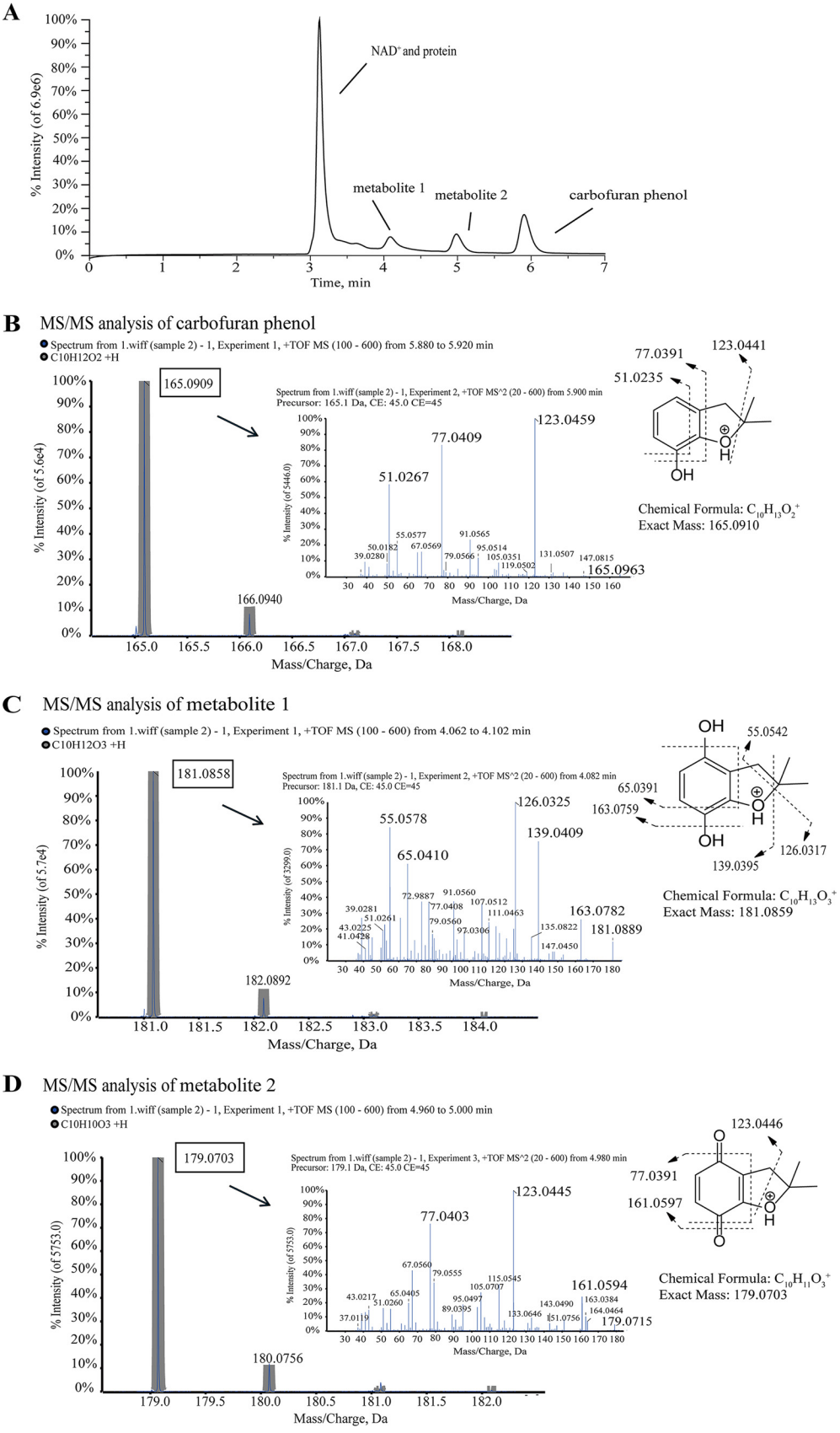

FIG 4 HPLC and MS/MS analyses of the products of carbofuran phenol treated with purified 6His-CfdC and CfdX-6His. (A) HPLC analysis of the products. The peak on the far left was also present in the control, which may be the peak of

(Continued on next page)

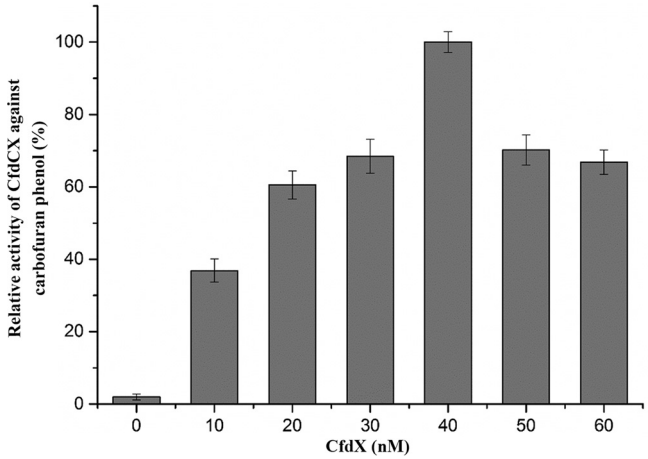

FIG 5 Relationship between the carbofuran phenol monooxygenase activity and various concentrations of CfdX-6His while the concentration of 6His-CfdC was kept constant. The concentration of CfdX-6His was increased from 0 to 0.06 μM, while the concentration of 6His-CfdC was kept constant at 1 μM. The 6His-CfdC specific activity against carbofuran phenol was defined as 100% when 0.04 μM CfdX-6His was added. Data were calculated from three independent replicates, and the error bars indicate standard deviations.

resonance was unsuccessful. The MS/MS analyses indicated that hydroxylation likely occurred at the *para* position (Fig. 4C). In addition, during the conversion of carbofuran phenol by strain CDS-1, the metabolites 1 and 2 were also detected and no benzene ring cleavage product of carbofuran phenol was found (data not shown).

DISCUSSION

Carbofuran has been widely used as an insecticide since 1967. To date, eight carbofuran-degrading sphingomonads have been described; all of these strains can transform carbofuran to carbofuran phenol and further convert carbofuran phenol (5–14). Two of these strains (CF06 and KN65.2) can grow on carbofuran (8, 13); only strain KN65.2 was reported to be able to mineralize the benzene ring of carbofuran (13). In this work, both genetic and biochemical results show that in strain CDS-1, $CehA_{CDS\text{-}1}$ hydrolyzes carbofuran to carbofuran phenol and $CfdC_{CDS\text{-}1}$ hydroxylates carbofuran phenol at the benzene ring. We assume that the close homologues of *cehA* and *cfdC* are present in all carbofuran-degrading sphingomonads and are responsible for the initial two steps of carbofuran catabolism.

The IS element plays an important role in the evolution of the catabolic pathway of xenobiotic compounds, and the involved genes are usually associated with an IS element (31). $cehA_{CDS\text{-}1}$ and $cfdC_{CDS\text{-}1}$ are linked to IS*6100*, while $cehA_{AC100}$ and $cehA_{KN65.2}$ are flanked by IS*Rsp3* (Fig. 1). The IS*6100* element is a member of the IS*6* family and has an extremely broad host range (32). IS*6100* has been found to be associated with the genes (*lin*, *mpd*, and *adoQTA1A2B*) involved in the catabolism of hexachlorocyclohexane, methyl parathion, and aniline (23, 33, 34). IS*Rsp3* containing a transposase gene pair (*istA*-*istB*) belongs to the IS*21* family (20). IS*Rsp3* is also adjacent to the chloroacetanilide *N*-dealkylase encoding gene *cndA* in *Sphingomonas* sp. strain DC-6 (35). The G+C contents of *cehA* (57.9%) and *cfdC* (60.5%) are obviously lower than those of the genomes of their host strains KN65.2 (63.1%) and CDS-1 (62.7%), showing the features of horizontal gene transfer. IS*6100* and IS*Rsp3* might contribute to the transposition of *cehA* and *cfdC*, facilitating the horizontal transfer of *cehA* and *cfdC*.

FIG 4 Legend (Continued)
NAD^+ or proteins added. The peaks of carbofuran phenol and two metabolites were further analyzed by tandem mass spectrometry (MS/MS) (B, C, and D). The mass spectra were collected using a TripleTOF 5600 (AB SCIEX) mass spectrometer. The metabolites were ionized by electrospray with positive polarity, and characteristic fragment ions were detected using MS/MS. The main fragment peaks are displayed with their chemical structures.

The unexpected finding of this study is that $CehA_{AC100}$ can hydrolyze carbofuran to carbofuran phenol, which is inconsistent with two previous reports (20, 21). Hashimoto et al. purified $CehA_{AC100}$ from the carbaryl-degrading strain AC100 and found that the purified $CehA_{AC100}$ showed no measurable activity against carbofuran (20). Öztürk et al. expressed $CehA_{AC100}$ and its four variants in *E. coli*; it should be noted that Öztürk et al. did not purify these five proteins, and the carbofuran hydrolytic activity assay was performed using cell extracts. The results indicate that $CehA_{AC100}$ could not transform carbofuran, and only the variants containing the Phe152Leu substitution can convert carbofuran to carbofuran phenol (21). Why the carbofuran-hydrolytic activity of $CehA_{AC100}$ was not detected in these two previous works may have two explanations. First, the HPLC retention times of carbofuran and carbofuran phenol are very close; neither the positive control nor the authentic chemical of carbofuran phenol was mentioned in the assay of $CehA_{AC100}$ purified from strain AC100 (20). Thus, if the HPLC peaks of carbofuran and carbofuran phenol could not be separated well, the generation of carbofuran phenol may be neglected. Second, $CehA_{AC100}$ is poorly expressed in *E. coli*; moreover, $CehA_{AC100}$ exhibits weak activity against carbofuran. If the soluble $CehA_{AC100}$ was present at only a very low concentration in the cell extracts, it would be difficult to detect its activity toward carbofuran. In this work, recombinant $CehA_{AC100}$ was purified to homogeneity. The result of the carbofuran-hydrolytic activity assay using the purified $CehA_{AC100}$ confirms that $CehA_{AC100}$ can convert carbofuran to carbofuran phenol. Additionally, in line with previous reports (21), we found that the Phe152Leu substitution significantly elevated the affinity and catalytic efficiency of $CehA_{AC100}$ against carbofuran.

Among the five putative flavin reductases tested, two supported the activity of CfdC. Furthermore, CfdC activity was also supported by the flavin reductases in *S. wittichii* RW1 and *P. putida* KT2440. However, the *E. coli* strains (DH5α or BL21) expressing CfdC failed to transform carbofuran phenol, indicating the flavin reductases of *E. coli* did not support the activity of CfdC. In strain DH5α, there is no flavin reductase gene present that is related to *cfdX* or CBW64_RS08340 (data not shown). These results show that CfdC has some degree of specificity in the recognition of its partner flavin reductase. This phenomenon has been described in other flavin-dependent monooxygenase systems (36–39). For example, the *E. coli* expressing only the oxygenase PheA1 of phenol hydroxylase PheA1A2 was unable to convert phenol, while coexpressing reductase PheA2 with PheA1 enabled the *E. coli* to convert phenol (36). Similarly, the *E. coli* cells synthesizing 2,5-diketocamphane monooxygenase (2,5-DKCMO) or 3,6-diketocamphane monooxygenase (3,6-DKCMO) without their cognate flavin reductase showed very little activity against camphor (37). In the absence of its partner reductase, MeaX that is involved in the catabolism of chloroacetanilide herbicides can be functionally expressed in strains *S. wittichii* RW1 and *P. putida* KT2440 but not in *E. coli* strains (DH5α or BL21) (38). Also, DszA that catalyzes the desulfurization of dibenzothiophene cannot be functionally expressed in *E. coli* (39). We postulate that some form of interaction between CfdC and its partner flavin reductase is required for the transfer of reduced FAD or FMN. The optimal ratio of 6His-CfdC and CfdX-6His is approximately 25:1, which is far less than that of phenol hydroxylase PheA1A2 (200:1) (40). *pheA1* and *pheA2* are organized in one operon in the genome of *Bacillus thermoglucosidasius* A7 (36), indicating that PheA1A2 is a well-evolved, two-component flavin-dependent monooxygenase system. In contrast, there was no evidence of a gene for a flavin reductase located in the immediate vicinity of *cfdC* in the genome of strain CDS-1. Although CfdX supported the activity of CfdC, CfdX is not the cognate reductase of CfdC; therefore, CfdCX is not a mature two-component monooxygenase system. Thus, PheA1 and PheA2 cooperate more efficiently than CfdC and CfdX.

The MS/MS data indicate that CfdCX hydroxylates the benzene ring of carbofuran phenol, likely at the *para* position. Notably, the MS/MS analyses show that this hydroxylation event does not result in the cleavage of the furanyl ring (Fig. 4C), which is different from previous speculations in strains KN65.2 and SB5 (10, 13). In strain KN65.2, the authors suggested that the *ortho* hydroxylation of the benzene ring of

TABLE 2 Strains and plasmids used in this study

Strain or plasmid	Characteristics[a]	Source or reference
Strains		
Sphingomonas sp.		
CDS-1	Wild type; able to convert carbofuran and carbofuran phenol; Str^r	CGMCC[b] 1025, 11
CDS-1-cehA	*cehA*-disrupted mutant of strain CDS-1; Str^r	This study
CDS-1-cfdC	*cfdC*-disrupted mutant of strain CDS-1; Str^r	This study
Pseudomonas putida KT2440	Wild type; unable to carbofuran or carbofuran phenol; Cm^r	26
Sphingomonas wittichii RW1	Wild type; unable to degrade carbofuran or carbofuran phenol; Str^r	25
Escherichia coli		
DH5α	F^- *recA1 endA1 thi-1 supE44 relA1 deoR* Δ(*lacZYA-argF*)*U169* ϕ80d*lacZ*ΔM15	TaKaRa
HB101(pRK600)	Conjugation helper strain; Cm^r	48
BL21(DE3)	F^- *ompT hsdS*(r_B^- m_B^-) *gal dcm lacY1* (DE3)	TaKaRa
Plasmids		
pJQ200SK	Mobilizable suicide vector; Gm^r	47
pJQKA	pJQ200SK containing the disruption construction of *cehA*; Gm^r	This study
pJQKC	pJQ200SK containing the disruption construction of *cfdC*; Gm^r	This study
pBBR1MCS-2	Broad-host-range cloning vector; Km^r	49
pBBR-A	pBBR1MCS-2 harboring *cehA*; Km^r	This study
pBBR-C	pBBR1MCS-2 harboring *cfdC*; Km^r	This study
pET28-ACDS	pET-28a(+) harboring $cehA_{CDS-1}$; Km^r	This study
pET28-AAC	pET-28a(+) harboring $cehA_{AC100}$; Km^r	This study
pET-28a(+)	Expression vector; Km^r	TaKaRa
pET07175	pET-28a(+) harboring gene CBW64_RS07175; Km^r	This study
pET07655	pET-28a(+) harboring gene CBW64_RS07655; Km^r	This study
pET08340	pET-28a(+) harboring gene CBW64_RS08340; Km^r	This study
pET14135	pET-28a(+) harboring gene CBW64_RS14135; Km^r	This study
pET17905 (same as pET-X)	pET-28a(+) harboring gene CBW64_RS17905; Km^r	This study
pET-C	pET-28a(+) harboring *cfdC*; Km^r	This study

[a]Str^r, streptomycin resistance; Cm^r, chloramphenicol resistance; Gm^r, gentamicin resistance; Km^r, kanamycin resistance.
[b]CGMCC, China General Microbiological Culture Collection Center.

carbofuran phenol by $CfdC_{KN65.2}$ led to the cleavage of the furanyl ring (Fig. 1A). In strain SB5, it was proposed that a putative hydrolase catalyzed the hydrolysis of the furanyl ring of carbofuran phenol. To explain these differences, genetic and biochemical evidence are required in both strains KN65.2 and SB5. In addition, since strain CDS-1 failed to grow on carbofuran or carbofuran phenol and no benzene ring cleavage product of carbofuran phenol was found during the conversion of carbofuran phenol by strain CDS-1 (data not shown), this strain lacks the genes for the downstream pathway of carbofuran catabolism, and these genes should be investigated in the sphingomonads that can mineralize carbofuran, such as strain KN65.2.

MATERIALS AND METHODS

Chemicals, bacterial strains, plasmids, and culture conditions. Carbofuran (97% purity) was kindly supplied by Jiangsu Kuaida Agrochemical Co., Ltd. Carbofuran phenol (99% purity) was purchased from Ehrenstorfer-Schafers (Augsburg, Germany). The stock solutions of carbofuran and carbofuran phenol were prepared in methanol and sterilized by membrane filtration (pore size, 0.22 μm). The bacterial strains and plasmids used in this study are listed in Table 2. All the bacterial strains were grown in Luria-Bertani (LB) medium. The *E. coli* strains were grown at 37°C, and other bacterial strains were grown at 30°C. Mineral salt medium (MSM; pH 7.0) contained the following (g/liter): NaCl, 1.0; NH_4NO_3, 1.0; K_2HPO_4, 1.5; KH_2PO_4, 0.5; $MgSO_4$, 0.1; and $CaCl_2{\cdot}2H_2O$, 0.1. The concentrations of various carbon sources supplemented in MSM are indicated in the experimental procedures section below. The following antibiotics were used for selections: streptomycin (Str), 100 μg/ml; ampicillin (Ap), 100 μg/ml; gentamicin (Gm), 30 μg/ml; chloramphenicol (Cm), 20 μg/ml; and kanamycin (Km), 50 μg/ml.

DNA manipulation, sequencing, and analysis. The isolation and manipulation of recombinant DNA were performed using standard techniques. All the enzymes were commercial preparations and were used as specified by the supplier (TaKaRa, Dalian, China). The oligonucleotides used in this study are listed in Table 3. The standard PCR mixture contained 10 μl PrimeSTAR buffer (5×), 4 μl deoxynucleoside triphosphate (dNTP) mix (2.5 mM each), 0.5 μM forward primer, 0.5 μM reverse primer, 10 ng template DNA, and 5 U PrimeSTAR HS DNA polymerase in a total volume of 50 μl; the cycling parameters were an initial denaturation at 98°C for 2 min and subsequent steps of 98°C for 10 s, annealing at 55 to 60°C for 10 s, and extension at 72°C for 1 min per kb, for 30 cycles total.

The total genomic DNA was extracted as described by Pitcher et al. (41). Genome sequencing was performed by Majorbio Bio-Pharm Technology Co., Ltd. (Shanghai, China). The draft genome sequence

TABLE 3 Oligonucleotides used in this study

Primer	Sequence (5′→3′)	Purpose
cehA-KO-F	TGCTCTAGAGCTAGGGTCACGCTCGAC	Construction of plasmid pJQKA
cehA-KO-R	CCGCTCGAGAAGACCTCGCCAACGGAG	
cehA-Com-F	CGGGGTACCGCGGTACGCGAACAAGCCG	Construction of plasmid pBBR-A
cehA-Com-R	CCGGAATTCTCACGTTAAGTCGCTTTCG	
cfdC-KO-F	TGCTCTAGACTCGGGCCCAGCAGACCG	Construction of plasmid pJQKC
cfdC-KO-R	CCGCTCGAGACCACGATGTCGTTGCTGC	
P1-F	CGGGGTACCCTCGCACGCGTGTCGACCG	Construction of plasmid pBBR-C
P1-R	CCGGAATTCGGTGGTCATCGGCTCTCT	
cfdC-F	CCGGAATTCATGGCAATTACCAAGCAG	
cfdC-R	CCCAAGCTTTTAGACCAGTGGATTATTC	
cehA-Ex-F	CAGCAAATGGGTCGCGGATCCTCGACTGACGCAATTGA	Construction of plasmids pET28-ACDS and pET28-AAC
cehA-Ex-R	TTGTCGACGGAGCTCGAATTCTCACGTTAAGTCGCTTTCGGC	
TTGC-R	CTGCTCAGCGGCGAACTTCGAGGCC	
TTGC-F	GGCCTCGAAGTTCGCCGCTGAGCAG	
07175-F	CGCCATATGATGAGCTTCAGGAAGGTGCTGG	Construction of plasmid pET07175
07175-R	CCGCTCGAGGAGCGCCAGAGGCGCGAACTG	
07655-F	CGCCATATGATGCAGTTCGACATGCGCGAGC	Construction of plasmid pET07655
07655-R	CCGCTCGAGTTCAGCCGCCTTGTCCTTGCCC	
17905-F	CGCCATATGACCGTCACGATCGACCCGCACG	Construction of plasmid pET17905
17905-R	CCGCTCGAGGATCGGCATGACCCGGCCATAGG	
14135-F	CGCCATATGATGCGATTCGACATGGCCGAGC	Construction of plasmid pET14135
14135-R	ATTTGCGGCCGCTATCCGGCTCTTCCCTCG	
08340-F	CGCCATATGATGAGCGAGGCGGGCAC	Construction of plasmid pET08340
08340-R	CCGCTCGAGGCCCAGATGGGCGAACTC	
cfdC-Ex-F	CATGCCATGGGCCACCACCACCACCACCACATGGCAATTACCAAGCAG	Construction of plasmid pET28a-C
cfdC-Ex-R	CCGGAATTCTTAGACCAGTGGATTATTCGGC	

of strain CDS-1 was produced using the Illumina MiSeq platform. The annotation was carried out using Glimmer 3.02 (42), tRNAscan-SE version 1.3.1 (43), and Barrnap 0.4.2 (44). BLASTN and BLASTP were used for the nucleotide sequence and deduced amino acid identity searches, respectively. To obtain the highly conserved genes between strains CDS-1 and KN65.2, the genome sequences of strain CDS-1 were searched against the genome of strain KN65.2 using BLASTN with default parameters; the BLASTN output was further filtered by an in-house PERL script using the strict criteria of alignment length of ≥100 bp, E value of <1e−5, and similarity of ≥95%. Then, the highly conserved sequences were retrieved with a filtered BLASTN output. For the phylogenetic analysis, Clustal X 2.1 (45) was used to align all the protein sequences. The multiple-sequence alignment was then imported into MEGA version 5.0 (46), and the phylogenetic tree was constructed by the neighbor-joining method.

Gene inactivation and complementation. To inactivate $cehA_{CDS\text{-}1}$ (GenBank gene locus tag CBW64_RS22415) through a single-crossover event, an 893-bp DNA fragment (in the middle of $cehA_{CDS\text{-}1}$) was generated by PCR using strain CDS-1 genomic DNA as the template and the primers cehA-KO-F and cehA-KO-R. The resulting product was then cloned between the XbaI and XhoI sites of the suicide plasmid pJQ200SK (47) to give pJQKA. pJQKA was delivered to strain CDS-1 via triparental mating (48), and the transconjugants were selected on LB plates supplemented with Str and Gm. The mutant strain CDS-1-cehA was confirmed by PCR and DNA sequencing. pBBR-A for gene complementation was constructed by ligating the fragment containing $cehA_{CDS\text{-}1}$ and its putative promoter region to the KpnI and EcoRI sites of the broad-host-range plasmid pBBR1MCS-2 (49). The plasmid was then transferred into mutant strain CDS-1-cehA via triparental mating. Similarly, *cfdC* (GenBank gene locus tag CBW64_RS25315) was inactivated using plasmid pJQKC, and the resulting mutant strain CDS-1-cfdC was complemented by plasmid pBBR-C.

Degradation test. The tested cells growing in LB broth overnight were washed twice with MSM and suspended in MSM containing 0.2 mM substrate to an optical density at 600 nm (OD_{600}) of approximately 1.0. The substrate and its metabolites were extracted by dichloromethane, and anhydrous sodium sulfate was used to dehydrate the organic phase. The solvent dichloromethane was removed by a stream of nitrogen gas, and the resulting samples were redissolved in methanol. After filtering through a 0.22-μm-pore Millipore membrane, the samples were analyzed using HPLC as described below.

Expression and purification of recombinant $CehA_{AC100}$ and $CehA_{CDS\text{-}1}$. The expression and purification of recombinant $cehA_{AC100}$ and $cehA_{CDS\text{-}1}$ were carried out according to a method described previously (21). To express *cehA* in *E. coli* BL21(DE3) using the pET-28a system, $cehA_{CDS\text{-}1}$ was amplified using primer pair cehA-Ex-F/cehA-Ex-R; since there is only single nucleotide transversion between $cehA_{AC100}$ and $cehA_{CDS\text{-}1}$, $cehA_{AC100}$ was generated by overlap PCR using primer pairs cehA-Ex-F/TTGC-R and TTGC-F/cehA-Ex-R with $cehA_{CDS\text{-}1}$ as the template. The N-terminal His-tagged $CehA_{AC100}$ and $CehA_{CDS\text{-}1}$ were purified on a Ni-nitrilotriacetic acid (NTA) agarose resin matrix (Sangon Biotech, Shanghai, China). The protein concentration was determined by the Bradford method (50) with bovine serum albumin as the standard.

Identification of a proper reductase component for $CfdC_{CDS\text{-}1}$. Five putative FMN/FAD reductase-encoding genes were predicted from the genome of strain CDS-1. The locus tags of these genes in the

GenBank database are CBW64_RS07175, CBW64_RS07655, CBW64_RS08340, CBW64_RS14135, and CBW64_RS17905. These five genes were ligated to plasmid pET-28a(+), producing pET07175, pET07655, pET08340, pET14135, and pET17905. Then, each of these five plasmids was introduced into *E. coli* BL21(DE3)/pBBR-C. The recombinant strains were grown to an OD_{600} of 0.5 before 0.2 mM IPTG (isopropyl-β-D-thiogalactopyranoside) was added. After 12 h of incubation at 16°C, the ability of the cells to convert carbofuran phenol was assayed as described above.

Synthesis and purification of recombinant CfdC and CfdX. The sequence of *cfdC* was PCR amplified using primers cfdC-F and cfdC-R and cloned into the expression vector pET-28a(+) to give pET-C. The plasmids pET-C and pET17905 were transferred into *E. coli* BL21(DE3) for protein expression and purification. When the OD_{600} reached approximately 0.5, 0.2 mM IPTG was added, and further cultivation was continued for 12 h at 16°C. The cells were harvested by centrifugation, suspended in binding buffer (20 mM Tris-HCl, 300 mM NaCl, 10 mM imidazole [pH 7.5]), and lysed by sonication. After centrifugation at 12,000 $\times$ *g* for 30 min at 4°C, the supernatant was charged onto a 1-cm^3 Ni-NTA gravity column (Sangon Biotech, Shanghai, China). After washing with washing buffer (20 mM Tris-HCl, 300 mM NaCl, 50 mM imidazole [pH 7.5]), the target proteins were eluted with 5 ml elution buffer (20 mM Tris-HCl, 300 mM NaCl, 500 mM imidazole [pH 7.5]). The purified protein was dialyzed against 20 mM Tris-HCl buffer (pH 7.5) and concentrated by ultrafiltration using the 10,000 molecular weight cutoff (MWCO) centrifugal filter (Merck Millipore, Germany). The purified proteins were detected by 12% sodium dodecyl sulfate-polyacrylamide gel electrophoresis (SDS-PAGE).

Enzyme assays. All the enzyme reactions were performed in Tris-HCl buffer (20 mM, pH 7.5) with a final volume of 1 ml. In the kinetic assays of $CehA_{AC100}$ and $CehA_{CDS-1}$ against carbofuran, seven concentrations of carbofuran (0.05, 0.1, 0.25, 0.5, 0.7, 1, and 1.25 mM) were added to the reaction mixtures. Each reaction mixture contained 28 nM purified protein. The reaction was performed at 30°C for 0, 10, 20, 30, 40, and 50 min and was terminated by adding 25 μl of 2 mM $HgCl_2$ (20). The consumption of carbofuran and the production of carbofuran phenol were analyzed by HPLC as described below.

NAD(P)H consumption at 340 nm was used for the determination of oxidoreductase activity of CfdX-6His. At this wavelength, the molar extinction coefficient for NAD(P)H was 6,220 $M^{-1} \cdot cm^{-1}$. In the kinetic assays of CfdX-6His, specific activities of CfdX for NADH were measured at nine concentrations of NADH (1, 3, 5, 10, 20, 40, 60, 80, and 100 μM) in the presence of 10 μM FMN/FAD (for the determination of the kinetic parameters for NADH) or at nine concentrations of FMN/FAD (0.1, 0.3, 0.5, 1, 3, 5, 7, 10, and 15 μM) in the presence of 200 μM NADH (for the determination of the kinetic parameters for FMN/FAD). In each of these assays, 9 nM CfdX-6His was used; the reactions were started by the addition of NAD(P)H, and the reaction mixtures were incubated at 30°C for 5, 10, 30, and 60 s.

To evaluate the relationship between the molar ratio of 6His-CfdC:CfdX-6His and carbofuran phenol hydroxylation activity, purified 6His-CfdC was kept constant at 1 μM, while the concentration of CfdX-6His increased from 0 to 0.06 μM. The concentration of carbofuran phenol was 250 μM. The reaction mixture was incubated at 30°C for 10 min and stopped by adding an equal volume of dichloromethane. To test the activity of recombinant CfdCX against carbofuran phenol, seven concentrations of substrate (25, 50, 70, 100, 150, 250, and 500 μM) were used in the presence of 200 μM NADH, 10 μM FMN/FAD, 1 μM 6His-CfdC, and 0.04 μM CfdX-6His. The reaction mixture was incubated at 30°C for 5, 10, and 15 min, and the reaction was stopped by adding an equal volume of dichloromethane. Carbofuran phenol in the organic phase was analyzed by HPLC. The products in the water phase and organic phase were detected by HPLC and MS/MS, as described below.

The kinetic data were evaluated by a nonlinear regression analysis with the Michaelis-Menten equation $v = V_{max} \times [S]/(K_m + [S])$, where v is the reaction rate and [S] is the concentration of substrate; the k_{cat} was calculated using the equation $V_{max} = k_{cat} \times$ [total enzyme concentration]. All the data were collected from three independent determinations. One unit of enzyme activity was defined as the amount of enzyme required to catalyze 1 μmol substrate per min at 30°C.

Analytical methods. The prepared samples were filtered through a 0.22-μm-pore Millipore membrane before HPLC analysis. The analysis was carried out as follows: the separation column was Shim-pack VP-ODS C_{18} (250 mm by 4.6 mm), the mobile phase was methanol/water at an 80:20 (vol/vol) ratio with a flow rate of 1.0 ml/min, and an SPD-20A detector was used to measure the UV absorption at 280 nm. The mass spectrum data were collected using a TripleTOF 5600 (AB SCIEX) mass spectrometer. The metabolites were ionized by electrospray with positive polarity, and characteristic fragment ions were detected using MS/MS.

Accession number(s). The draft genome sequence of *Sphingomonas* sp. CDS-1 has been deposited in the GenBank database under accession number NHRH00000000.

SUPPLEMENTAL MATERIAL

Supplemental material for this article may be found at https://doi.org/10.1128/AEM.00805-18.

SUPPLEMENTAL FILE 1, PDF file, 0.5 MB.

ACKNOWLEDGMENTS

We thank Jun Wu (Nanjing Agricultural University) for help in the analysis of the intermediate metabolites.

This work was supported by the National Natural Science Foundation of China (31670112,

31370155, 31470225), the National Key R&D Program of China (SQ2017YFNC060022-02), the Jiangsu Agriculture Science and Technology Innovation Fund CX (15)1004, and the Fundamental Research Funds for the Central Universities (KYZ201528).

REFERENCES

1. Chapalamadugu S, Chaudhry GR. 1992. Microbiological and biotechnological aspects of metabolism of carbamates and organophosphates. Crit Rev Biotechnol 12:357–389. https://doi.org/10.3109/07388559209114232.
2. Fahmy MA, Fukuto TR, Myers RO, March RB. 1970. The selective toxicity of new *N*-phosphorothioyl-carbamate esters. J Agric Food Chem 18:793–796. https://doi.org/10.1021/jf60171a014.
3. Gupta RC. 1994. Carbofuran toxicity. J Toxicol Environ Health 43:383–418. https://doi.org/10.1080/15287399409531931.
4. Goad RT, Goad JT, Atieh BH, Gupta RC. 2004. Carbofuran-induced endocrine disruption in adult male rats. Toxicol Mech Methods 14:233–239. https://doi.org/10.1080/15376520490434476.
5. Chaudhry GR, Ali AN. 1988. Bacterial metabolism of carbofuran. Appl Environ Microbiol 54:1414–1419.
6. Desaint S, Arrault S, Siblot S, Fournier JC. 2003. Genetic transfer of the *mcd* gene in soil. J Appl Microbiol 95:102–108. https://doi.org/10.1046/j.1365-2672.2003.01965.x.
7. Karns JS, Mulbry WW, Nelson JO, Kearney PC. 1986. Metabolism of carbofuran by a pure bacterial culture. Pestic Biochem Physiol 25:211–217. https://doi.org/10.1016/0048-3575(86)90048-9.
8. Feng X, Ou LT, Ogram A. 1997. Plasmid-mediated mineralization of carbofuran by *Sphingomonas* sp. strain CF06. Appl Environ Microbiol 63:1332–1337.
9. Ogram AV, Duan YP, Trabue SL, Feng X, Castro H, Ou LT. 2000. Carbofuran degradation mediated by three related plasmid systems. FEMS Microbiol Ecol 32:197–203. https://doi.org/10.1111/j.1574-6941.2000.tb00712.x.
10. Kim IS, Ryu JY, Hur HG, Gu MB, Kim SD, Shim JH. 2004. *Sphingomonas* sp. strain SB5 degrades carbofuran to a new metabolite by hydrolysis at the furanyl ring. J Agric Food Chem 52:2309–2314. https://doi.org/10.1021/jf035502l.
11. Wu J, Xu JH, Hong Q, Liu Z, Zhang XH, Li SP. 2004. Isolation of a carbofuran degrading bacterium (CDS-1) and its characterization. Huanjing Kexue Xuebao 24:338–342. (In Chinese.)
12. Yan QX, Hong Q, Han P, Dong XJ, Shen YJ, Li SP. 2007. Isolation and characterization of a carbofuran-degrading strain *Novosphingobium* sp. FND-3. FEMS Microbiol Lett 271:207–213. https://doi.org/10.1111/j.1574-6968.2007.00718.x.
13. Nguyen TP, Helbling DE, Bers K, Fida TT, Wattiez R, Kohler HP, Springael D, De Mot R. 2014. Genetic and metabolic analysis of the carbofuran catabolic pathway in *Novosphingobium* sp. KN65.2. Appl Microbiol Biotechnol 98:8235–8252. https://doi.org/10.1007/s00253-014-5858-5.
14. Peng X, Zhang JS, Li YY, Li W, Xu GM, Yan YC. 2008. Biodegradation of insecticide carbofuran by *Paracoccus* sp. YM3. J Environ Sci Health B 43:588–594. https://doi.org/10.1080/03601230802234492.
15. Balkwill DL, Fredrickson JK, Romine MF. 2006. *Sphingomonas* and related genera, p 605–629. *In* Dworkin M (ed), The prokaryotes: an evolving electronic resource for the microbiological community, vol 7. Springer-Verlag, New York, NY.
16. Takeuchi M, Hamana K, Hiraishi A. 2001. Proposal of the genus *Sphingomonas sensu stricto* and three new genera, *Sphingobium*, *Novosphingobium* and *Sphingopyxis*, on the basis of phylogenetic and chemotaxonomic analyses. Int J Syst Evol Microbiol 51:1405–1417. https://doi.org/10.1099/00207713-51-4-1405.
17. Tomasek PH, Karns JS. 1989. Cloning of a carbofuran hydrolase gene from *Achromobacter* sp. strain WM111 and its expression in gram-negative bacteria. J Bacteriol 171:4038–4044. https://doi.org/10.1128/jb.171.7.4038-4044.1989.
18. Parekh NR, Hartmann A, Charnay MP, Fournier JC. 1995. Diversity of carbofuran-degrading soil bacteria and detection of plasmid-encoded sequences homologous to the *mcd* gene. FEMS Microbiol Ecol 17:149–160. https://doi.org/10.1111/j.1574-6941.1995.tb00138.x.
19. Nguyen TP, De Mot R, Springael D. 2015. Draft genome sequence of the carbofuran-mineralizing *Novosphingobium* sp. strain KN65.2. Genome Announc 3:e00764-15. https://doi.org/10.1128/genomeA.00764-15.
20. Hashimoto M, Fukui M, Hayano K, Hayatsu M. 2002. Nucleotide sequence and genetic structure of a novel carbaryl hydrolase gene (*cehA*) from *Rhizobium* sp. strain AC100. Appl Environ Microbiol 68:1220–1227. https://doi.org/10.1128/AEM.68.3.1220-1227.2002.
21. Öztürk B, Ghequire M, Nguyen TP, De Mot R, Wattiez R, Springael D. 2016. Expanded insecticide catabolic activity gained by a single nucleotide substitution in a bacterial carbamate hydrolase gene. Environ Microbiol 18:4878–4887. https://doi.org/10.1111/1462-2920.13409.
22. Lal R, Dogra C, Malhotra S, Sharma P, Pal R. 2006. Diversity, distribution and divergence of *lin* genes in hexachlorocyclohexane-degrading sphingomonads. Trends Biotechnol 24:121–130. https://doi.org/10.1016/j.tibtech.2006.01.005.
23. Yan X, Gu T, Yi Z, Huang J, Liu X, Zhang J, Xu X, Xin Z, Hong Q, He J. 2016. Comparative genomic analysis of isoproturon-mineralizing sphingomonads reveals the isoproturon catabolic mechanism. Environ Microbiol 18:4888–4906. https://doi.org/10.1111/1462-2920.13413.
24. Park MR, Lee S, Han TH, Oh BT, Shim JH, Kim IS. 2006. A new intermediate in the degradation of carbofuran by *Sphingomonas* sp. strain SB5. J Microbiol Biotechnol 16:1306–1310.
25. Wittich RM, Wilkes H, Sinnwell V, Francke W, Fortnagel P. 1992. Metabolism of dibenzo-*p*-dioxin by *Sphingomonas* sp. strain RW1. Appl Environ Microbiol 58:1005–1010.
26. Nelson KE, Weinel C, Paulsen IT, Dodson RJ, Hilbert H, Martins dos Santos VA, Fouts DE, Gill SR, Pop M, Holmes M, Brinkac L, Beanan M, DeBoy RT, Daugherty S, Kolonay J, Madupu R, Nelson W, White O, Peterson J, Khouri H, Hance I, Chris Lee P, Holtzapple E, Scanlan D, Tran K, Moazzez A, Utterback T, Rizzo M, Lee K, Kosack D, Moestl D, Wedler H, Lauber J, Stjepandic D, Hoheisel J, Straetz M, Heim S, Kiewitz C, Eisen JA, Timmis KN, Düsterhöft A, Tümmler B, Fraser CM. 2002. Complete genome sequence and comparative analysis of the metabolically versatile *Pseudomonas putida* KT2440. Environ Microbiol 4:799–808. https://doi.org/10.1046/j.1462-2920.2002.00366.x.
27. Huijbers MM, Montersino S, Westphal AH, Tischler D, van Berkel WJ. 2014. Flavin dependent monooxygenases. Arch Biochem Biophys 544:2–17. https://doi.org/10.1016/j.abb.2013.12.005.
28. Sucharitakul J, Chaiyen P, Entsch B, Ballou DP. 2006. Kinetic mechanisms of the oxygenase from a two-component enzyme, *p*-hydroxyphenylacetate 3-hydroxylase from *Acinetobacter baumannii*. J Biol Chem 281:17044–17053. https://doi.org/10.1074/jbc.M512385200.
29. Chakraborty S, Ortiz-Maldonado M, Entsch B, Ballou DP. 2010. Studies on the mechanism of *p*-hydroxyphenylacetate 3-hydroxylase from *Pseudomonas aeruginosa*: a system composed of a small flavin reductase and a large flavin-dependent oxygenase. Biochemistry 49:372–385. https://doi.org/10.1021/bi901454u.
30. Blake SL, Walker SH, Muddiman DC, Hinks D, Beck KR. 2011. Spectral accuracy and sulfur counting capabilities of the LTQ-FT-ICR and the LTQ-Orbitrap XL for small molecule analysis. J Am Soc Mass Spectrom 22:2269–2275. https://doi.org/10.1007/s13361-011-0244-3.
31. Ochman H, Lawrence JG, Groisman EA. 2000. Lateral gene transfer and the nature of bacterial innovation. Nature 405:299–304. https://doi.org/10.1038/35012500.
32. Mahillon J, Chandler M. 1998. Insertion sequences. Microbiol Mol Biol Rev 62:725–774.
33. Verma H, Kumar R, Oldach P, Sangwan N, Khurana JP, Gilbert JA, Lal R. 2014. Comparative genomic analysis of nine *Sphingobium* strains: insights into their evolution and hexachlorocyclohexane (HCH) degradation pathways. BMC Genomics 15:1014. https://doi.org/10.1186/1471-2164-15-1014.
34. Zhang R, Cui Z, Zhang X, Jiang J, Gu JD, Li S. 2006. Cloning of the organophosphorus pesticide hydrolase gene clusters of seven degradative bacteria isolated from a methyl parathion contaminated site and evidence of their horizontal gene transfer. Biodegradation 17:465–472. https://doi.org/10.1007/s10532-005-9018-6.
35. Chen Q, Wang CH, Deng SK, Wu YD, Li Y, Yao L, Jiang JD, Yan X, He J, Li SP. 2014. Novel three-component Rieske non-heme iron oxygenase system catalyzing the *N*-dealkylation of chloroacetanilide herbicides in *Sphingomonads* DC-6 and DC-2. Appl Environ Microbiol 80:5078–5085. https://doi.org/10.1128/AEM.00659-14.

36. Duffner FM, Kirchner U, Bauer MP, Müller R. 2000. Phenol/cresol degradation by the thermophilic *Bacillus thermoglucosidasius* A7: cloning and sequence analysis of five genes involved in the pathway. Gene 256: 215–221. https://doi.org/10.1016/S0378-1119(00)00352-8.
37. Iwaki H, Grosse S, Bergeron H, Leisch H, Morley K, Hasegawa Y, Lau PC. 2013. Camphor pathway redux: functional recombinant expression of 2,5- and 3,6-diketocamphane monooxygenases of *Pseudomonas putida* ATCC 17453 with their cognate flavin reductase catalyzing Baeyer-Villiger reactions. Appl Environ Microbiol 79:3282–3293. https://doi.org/10.1128/AEM.03958-12.
38. Cheng M, Meng Q, Yang Y, Chu C, Chen Q, Li Y, Cheng D, Hong Q, Yan X, He J. 2017. The two-component monooxygenase MeaXY initiates the downstream pathway of chloroacetanilide herbicide catabolism in sphingomonads. Appl Environ Microbiol 83:e03241-16. https://doi.org/10.1128/AEM.03241-16.
39. Gray KA, Pogrebinsky OS, Mrachko GT, Xi L, Monticello DJ, Squires CH. 1996. Molecular mechanisms of biocatalytic desulfurization of fossil fuels. Nat Biotechnol 14:1705–1709. https://doi.org/10.1038/nbt1296-1705.
40. Kirchner U, Westphal AH, Müller R, van Berkel WJ. 2003. Phenol hydroxylase from *Bacillus thermoglucosidasius* A7, a two-protein component monooxygenase with a dual role for FAD. J Biol Chem 278:47545–47553. https://doi.org/10.1074/jbc.M307397200.
41. Pitcher DG, Saunders NA, Owen RJ. 1989. Rapid extraction of bacterial genomic DNA with guanidium thiocyanate. Lett Appl Microbiol 8:151–156. https://doi.org/10.1111/j.1472-765X.1989.tb00262.x.
42. Delcher AL, Bratke KA, Powers EC, Salzberg SL. 2007. Identifying bacterial genes and endosymbiont DNA with Glimmer. Bioinformatics 23: 673–679. https://doi.org/10.1093/bioinformatics/btm009.
43. Lowe TM, Eddy SR. 1997. tRNAscan-SE: a program for improved detection of transfer RNA genes in genomic sequence. Nucleic Acids Res 25:955–964. https://doi.org/10.1093/nar/25.5.0955.
44. Lagesen K, Hallin P, Rødland EA, Staerfeldt HH, Rognes T, Ussery DW. 2007. RNAmmer: consistent and rapid annotation of ribosomal RNA genes. Nucleic Acids Res 35:3100–3108. https://doi.org/10.1093/nar/gkm160.
45. Larkin MA, Blackshields G, Brown N, Chenna R, McGettigan PA, McWilliam H, Valentin F, Wallace IM, Wilm A, Lopez R, Gibson TJ, Higgins DG. 2007. Clustal W and Clustal X version 2.0. Bioinformatics 23:2947–2948. https://doi.org/10.1093/bioinformatics/btm404.
46. Tamura K, Peterson D, Peterson N, Stecher G, Nei M, Kumar S. 2011. MEGA5: molecular evolutionary genetics analysis using maximum likelihood, evolutionary distance, and maximum parsimony methods. Mol Biol Evol 28:2731–2739. https://doi.org/10.1093/molbev/msr121.
47. Quandt J, Hynes MF. 1993. Versatile suicide vectors which allow direct selection for gene replacement in Gram-negative bacteria. Gene 127: 15–21. https://doi.org/10.1016/0378-1119(93)90611-6.
48. Herrero M, De LV, Timmis KN. 1990. Transposon vectors containing non-antibiotic resistance selection markers for cloning and stable chromosomal insertion of foreign genes in Gram-negative bacteria. J Bacteriol 172:6557–6567. https://doi.org/10.1128/jb.172.11.6557-6567.1990.
49. Kovach ME, Elzer PH, Hill DS, Robertson GT, Farris MA, Roop RM, Peterson KM. 1995. Four new derivatives of the broad-host-range cloning vector pBBR1MCS, carrying different antibiotic-resistance cassettes. Gene 166:175–176. https://doi.org/10.1016/0378-1119(95)00584-1.
50. Bradford MM. 1976. A rapid and sensitive method for the quantitation of microgram quantities of protein utilizing the principle of protein-dye binding. Anal Biochem 72:248–254. https://doi.org/10.1016/0003-2697(76)90527-3.